The International Journal of Advanced Manufacturing Technology (2018) 96:2747–2755
https://doi.org/10.1007/s00170-018-1789-0

ORIGINAL ARTICLE

Ultrasonic strengthening improves tensile mechanical performance of fused deposition modeling 3D printing

Guiwei Li[1] · Ji Zhao[1] · Jili Jiang[1] · Hao Jiang[1] · Wenzheng Wu[1] · Mengxin Tang[1]

Received: 5 November 2017 / Accepted: 12 February 2018 / Published online: 24 February 2018
© Springer-Verlag London Ltd., part of Springer Nature 2018

Abstract
Wire-by-wire and layer-by-layer printing processes used in fused deposition modeling (FDM) three-dimensional (3D) printed parts result in poor mechanical properties. In this study, 3D printed acrylonitrile butadiene styrene (ABS) samples strengthened by ultrasonic vibrations are studied by a controlled variate method. The effects of ultrasonic strengthening pressure and ultrasonic strengthening time on the tensile mechanical properties of samples are studied. The tensile strength of the samples increases by 11.3%, the Young's modulus increases by 16.7%, and the surface roughness decreases after ultrasonic strengthening. Ultrasonic strengthening after FDM 3D printing significantly improves the tensile mechanical properties of the sample and broadens the potential applications for FDM 3D printing technology.

Keywords 3D printing · Ultrasonic strengthening · Fused deposition modeling · Additive manufacturing

1 Introduction

Fused deposition modeling (FDM) is a three-dimensional (3D) printing technology in which filamentous materials are heated or melted and deposited in layers to build up the 3D sample. The material is deposited onto the work surface by a nozzle, which is controlled by computer according to the 3D design [1]. Because of its rapid fabrication speed, simple process, low manufacturing cost, and capability of directly fabricating complex solid parts, FDM has become the most widely used additive manufacturing technology [2–6]. However, defects can be caused by the progressive and cumulative process of FDM, such as unintended voids or bonds between rasters. Compared with injection molded parts, FDM 3D printed samples have poor comprehensive mechanical properties, limiting the potential applications of such parts [7, 8]. Therefore, it is very important to improve the mechanical properties of FDM 3D printed parts [9–11].

Many studies have investigated improvements to the mechanical properties of FDM 3D printed samples. The effect of adding carbon fiber to acrylonitrile butadiene styrene (ABS) on the mechanical properties of 3D printed samples has been studied by Ning et al. [12]. The effect of continuous fiber reinforcement on the mechanical properties of 3D printed samples has also been studied by Tian et al. [13]. Nikzad et al. found that adding iron or copper to ABS composites gives 3D printed samples better rigidity and flexibility [14]. By adding montmorillonite into ABS, Weng et al. found that the elastic modulus of 3D printed samples was significantly improved [15]. Lederle et al. found that 3D printing ABS samples in a nitrogen atmosphere inhibits the oxidation of ABS during the printing process, thereby improving the mechanical properties of printed samples [16]. Mohamed et al. studied the influence of melt deposition angle and direction on the mechanical properties of 3D printed ABS samples [17]. These studies mainly focused on improving the mechanical properties of FDM 3D printed samples by modifying the printing materials or changing the printing process.

Ultrasonic plastic welding involves focusing ultrasonic vibrations through a horn onto a joint to be welded. Under certain pressure, these vibrations cause the two plastic parts in contact to experience friction and deformation, which will result in temperature rise and the two surfaces in contact weld

Electronic supplementary material The online version of this article (https://doi.org/10.1007/s00170-018-1789-0) contains supplementary material, which is available to authorized users.

✉ Wenzheng Wu
wzwu@jlu.edu.cn

[1] School of Mechanical Science and Engineering, Jilin University, Renmin Street 5988, Changchun, Jilin 130025, China

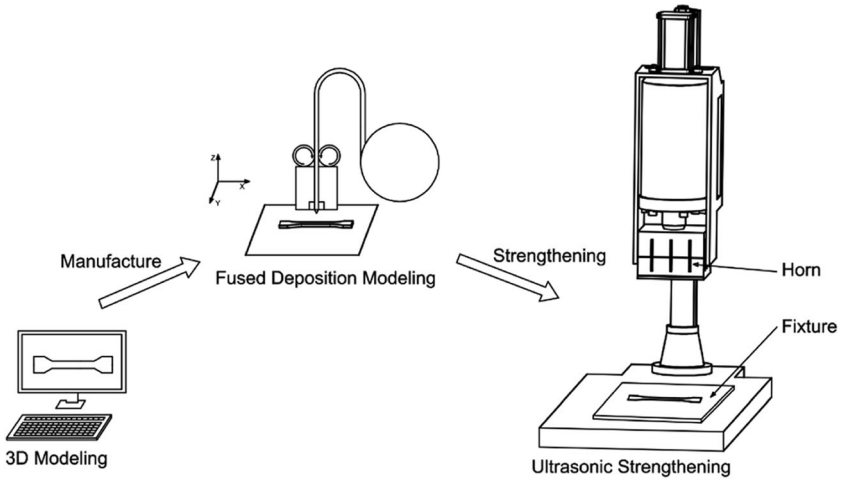

Fig. 1 Ultrasonic strengthening 3D printing process

together [18]. In the present study, based on the principle of ultrasonic plastic welding, an ultrasonic strengthening system is designed. Under certain pressure, ultrasonic vibrations can strengthen the bonding among the deposited rasters and the deposited layers, which will improve the mechanical properties of the 3D printed samples.

FDM 3D printed ABS samples with impact resistance, heat resistance, low temperature resistance, chemical resistance, and excellent electrical properties, the characteristics of product size stability, good surface gloss, are widely used in machinery, automobile, electronic and electrical appliances, instruments, textile, and architecture [19–22]. In this study, the tensile mechanical properties of ultrasonic strengthened 3D printed ABS samples taken as an example, the principle of improving the mechanical properties of 3D printed samples by FDM technology is studied through experiments.

2 Experimental methods

The ultrasonic strengthening 3D printing process is shown in Fig. 1. The part was designed using 3D modeling software on a computer, and samples were 3D printed. The ultrasonic strengthening system was employed to strengthen the 3D printed sample and to enhance its mechanical properties.

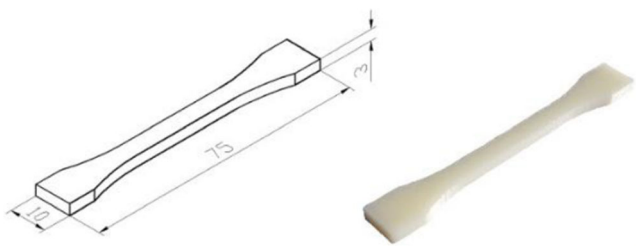

Fig. 2 Tensile mechanical sample

2.1 3D printed tensile mechanical samples

Designed according to GB/T 16421-1996, an example of the 3D printed samples is shown in Fig. 2. CATIA V5 software was used for 3D modeling and a uPrint SE 3D printer was used for FDM. The printing material was ABS plusTM-P430 and the support material was SR-30 soluble support. The printing layer thickness was 0.254 mm, the printing speed was 15 mm/s, and the interior of the sample was completely filled.

2.2 Ultrasonic strengthening of 3D printed samples

Under static pressure, the ultrasonic vibration system transfers ultrasonic vibration energy to the internal parts of the 3D printed sample, and then transforms into the friction energy of the internal bond of the sample. The friction energy is transformed into heat energy and deformation energy in the process of ultrasonic strengthening, so as to realize fusion of broken rasters.

In the process of ultrasonic strengthening, the relative friction speed v between the internal rasters of 3D printed samples is as follows:

$$v = \frac{2Aw}{\pi} = \frac{2A(2\pi f)}{\pi} = 4Af, \tag{1}$$

where V is the relative friction velocity, A is the amplitude, w is the angular frequency, and f is the frequency.

The power P of the friction motion between rasters is as follows:

$$P = SFkv, \tag{2}$$

Table 1 Experimental scheme

Group	Factor	Level									Unit
A	Time	0.25	0.30	0.35	0.40	0.45	0.50	0.55	0.60	0.65	s
	Pressure	3.5									kg/cm^2
B	Time	0.5									s
	Pressure		2	2.5	3	3.5	4	4.5	5		kg/cm^2

where S is the contact area between the ultrasonic strengthening system and the 3D printed sample, F is the strengthening pressure, and k is the coefficient of friction.

The energy input Q from the ultrasonic strengthening system to the 3D printed sample is as follows:

$$Q = Pt, \tag{3}$$

where t is the ultrasonic strengthening time. Combining (1), (2), and (3) gives the following:

$$Q = 4ASFkft. \tag{4}$$

This shows that the energy input from ultrasonic strengthening system to the 3D printed sample is positively correlated with A, S, F, k, f, and t. The experimental results show that the ultrasonic strengthening parameters A, S, k, and F are almost fixed values for certain ultrasonic strengthening systems and for certain materials; thus, these have a small effect on the input energy. Therefore, in the present study, the effect of F and t on the mechanical properties of ultrasonic strengthened 3D printed samples is studied. The experimental scheme is shown in Table 1.

In the present study, FDM 3D printed ABS samples were reinforced with a customized ultrasonic strengthening system. The power output of the ultrasonic strengthening system was 2 kW, the frequency was 20 kHz, the delay time was 0.35 s, and the hold time was 0.4 s. The ultrasonic strengthening process is shown in Fig. 3. First, the samples were fixed to the work surface, and the ultrasonic strengthening system was set up using appropriate parameters in the start position. Then, the ultrasonic horn was lowered to be in contact with the sample. The horn applied pressure and ultrasonic vibrations to the sample to strengthen it. After strengthening, the horn remained in contact with the sample for some time to prevent warping. Finally, the horn was separated from the sample and returned to the start position.

2.3 Tensile property test of ultrasonic strengthened samples

The 3D printed ABS samples were tested using the INSTRON 5982 electronic universal testing machine. Five samples were strengthened according to the experimental parameters of each group, taking the average value of the tensile test as the mechanical property for the samples. Five untreated samples were also tested, to compare and analyze the effect of the ultrasonic strengthening process. The fracture characteristics of tensile fracture specimens were observed by digital microscope VHX-900 (KEYENCE, Japan) to observe the surface morphology of the samples after ultrasonic strengthening.

3 Results and discussion

3.1 Effect of ultrasonic strengthening on tensile properties of 3D printed samples

Figure 4 and Fig. 5 show the stress–strain curves of the 3D printed samples. The tensile properties of the strengthened samples were improved by increasing the ultrasonic strengthening time or increasing the ultrasonic strengthening pressure. Figure 6 shows the fractured samples when the ultrasonic strengthening pressure was 3.5 kg/cm^2. Figure 7 shows fractured samples when the ultrasonic strengthening time was 0.5 s. All fractures are normal, showing that energy was dispersed evenly within the 3D printed samples.

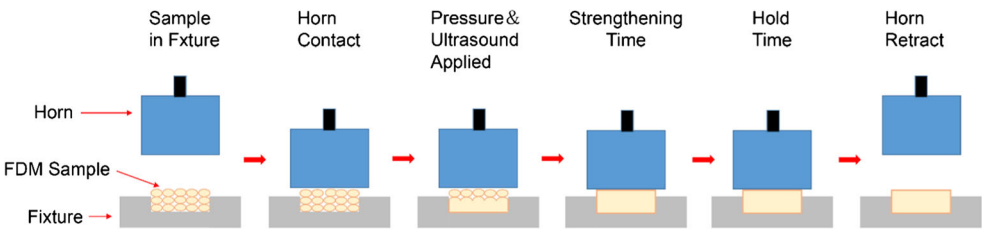

Fig. 3 Ultrasonic strengthening process

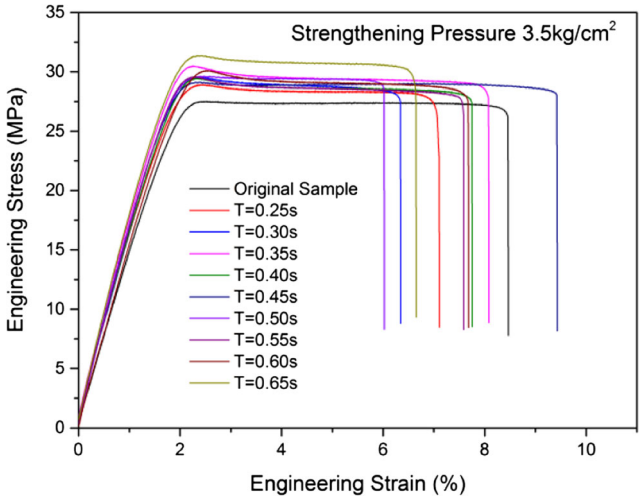

Fig. 4 Stress–strain diagram under ultrasonic strengthening pressure of 3.5 kg/cm^2

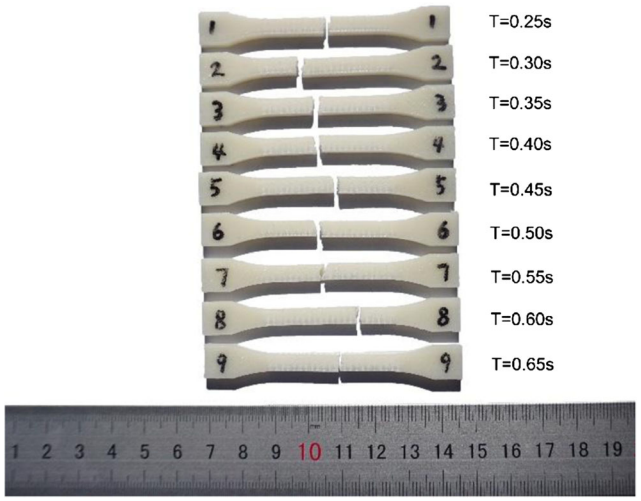

Fig. 6 Tensile fracture of 3D printed samples under strengthening pressure of 3.5 kg/cm^2

3.2 Effect of ultrasonic strengthening on tensile strength

Figure 8 and Fig. 9 are curves of tensile strength with ultrasonic strengthening parameters. The tensile strength of the strengthened 3D printed samples was improved by up to 11.3% compared with that of untreated samples. It can be seen from Fig. 8 that with increasing ultrasonic strengthening time, the tensile strength increases, although there is a decrease from 3.5 to 4.5 s.

As it is shown in Fig. 3, under static pressure, the ultrasonic vibration energy is transmitted from horn, through the surface it is in contact with, then through the sample to the work surface. Where there are a 3D printing defects, adjacent rasters begin to rub, deform, heat up, and then fuse together. With increasing energy input, the fusion zone grows, enhancing the tensile strength of the sample.

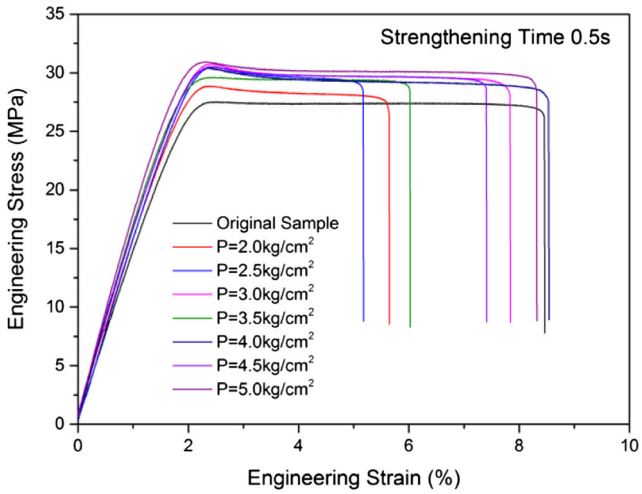

Fig. 5 Stress–strain diagram under ultrasonic strengthening time of 0.5 s

Because the ultrasonic vibration energy is transferred from the contact surface to the interior, on the contact surface, where the bonding of the rasters is not firm or there is a printing defect, the rasters are in the state of vibration with no fixture, under the influence of continuous ultrasonic vibration, the printing defects continue to expand. With the increase of ultrasonic action time, the fusion zone expands and the damage zone shrinks. Therefore, with the increase of ultrasonic strengthening time, the vibration energy input increases gradually, and the ultrasonic strengthening area gradually increases, and the curve shows an upward trend as a whole. In the process of ultrasonic strengthening, in the fusion zone far away from the contact surface, with the increase of ultrasonic action time, the crack of the rasters around the contact surface is easy to crack as the tensile force increases. With the propagation of the crack, the sample reaches the tensile limit and is broken. Therefore, with the increase of strengthening time, the curve will appear a downward trend, but it still plays a strengthening role in the whole samples. As the fusion zone

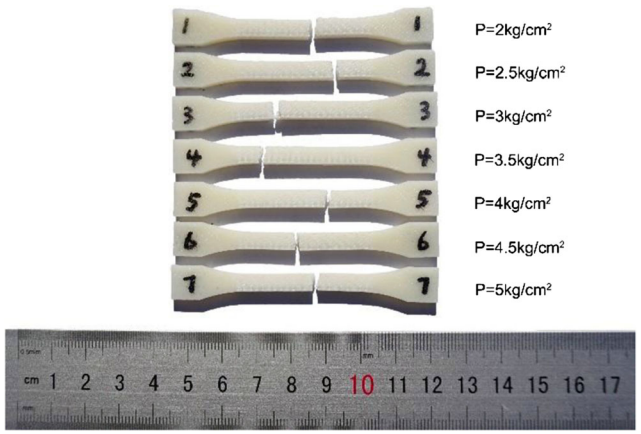

Fig. 7 Tensile fracture of 3D printed samples under strengthening time of 0.5 s

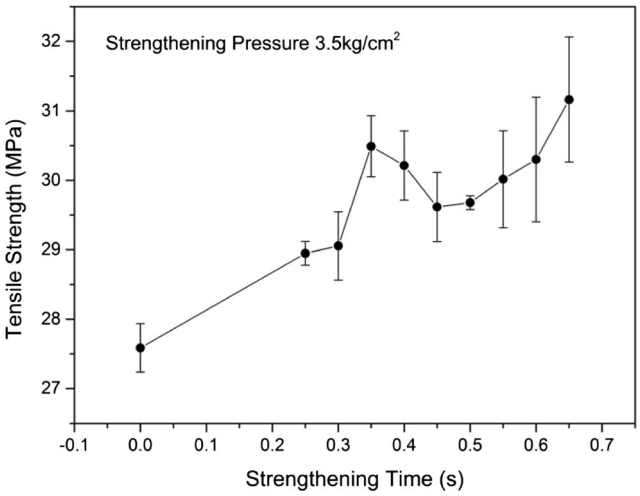

Fig. 8 Stress–strain changes with time under ultrasonic strengthening pressure of 3.5 kg/cm^2

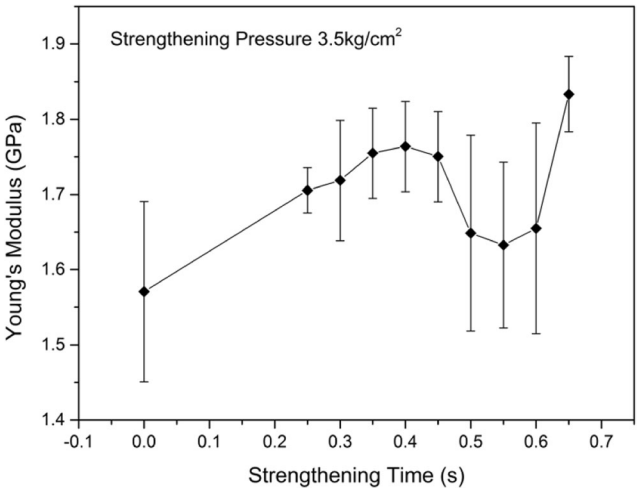

Fig. 10 Young's modulus changes with time under ultrasonic strengthening pressure of 3.5 kg/cm^2

grows closer to the contact surface, the internal defects of the 3D printed samples amplified by the ultrasonic vibration before are continuously fused and repaired. At this time, with the increase of ultrasonic strengthening time, the curve continues to show an upward trend.

It can be seen from Fig. 9 that, with increasing ultrasonic pressure, the tensile strength increases. With increasing ultrasonic pressure, the energy input from the ultrasonic strengthening system to the 3D printed sample increases gradually; thus, the tensile strength of the sample gradually increases. Similarly, owing to the presence of the transfer process of ultrasonic vibration energy in the 3D printed samples, the strengthening effect and damage effect exist simultaneously; while the curve rises in the process, there will be a peak.

Despite the results shown in Fig. 8 and Fig. 9, the ultrasonic vibration energy input to the 3D printed samples cannot be infinitely increased. When the energy input is too large, although the tensile strength of the sample is enhanced, the surface in contact with the horn is damaged, causing surface pasting or cloak phenomenon.

3.3 Effect of ultrasonic strengthening on Young's modulus

Figure 10 and Fig. 11 show Young's modulus of 3D printed samples for different ultrasonic strengthening parameters. The Young's modulus of strengthened samples improved by up to 16.7% compared with that of untreated samples. It can be seen from Fig. 10 that with increasing strengthening pressure, Young's modulus increases. There is a trough in the course of the curve rising, which means that the effect of the ultrasonic on Young's modulus is also twofold when the ultrasonic continues to act on the samples. For higher values of Young's modulus, the errors are smaller than those for lower values of

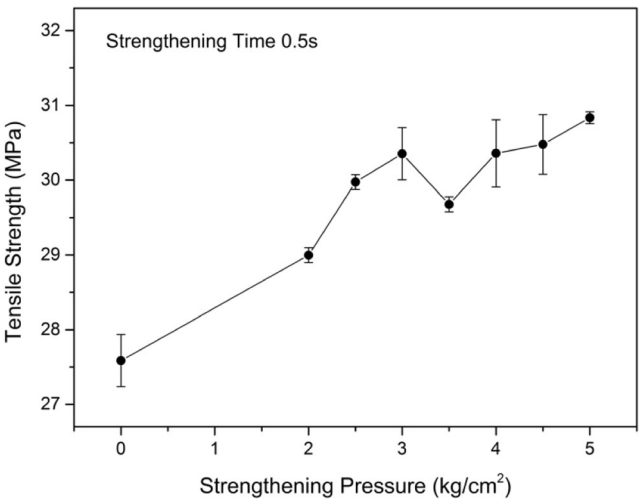

Fig. 9 Stress–strain changes with pressure under ultrasonic strengthening time of 0.5 s

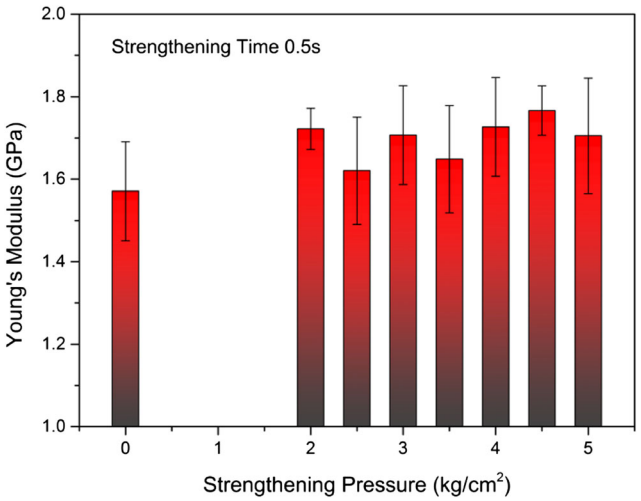

Fig. 11 Young's modulus changes with pressure under ultrasonic strengthening time of 0.5 s

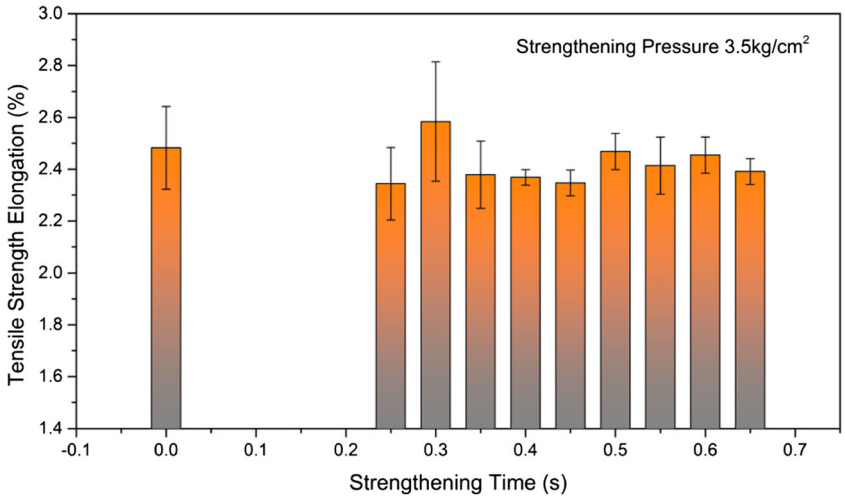

Fig. 12 Tensile elongation at ultrasonic strengthening pressure of 3.5 kg/cm^2

Young's modulus and for the untreated samples. This suggests that the elasticity of these samples is more stable. However, when Young's modulus is low, the elastic modulus error is relatively large, and the elastic stability is similar to that of untreated samples. It can be seen from Fig. 11 that with the increasing strengthening pressure, Young's modulus increases, and the errors are similar to those of untreated samples. When the ultrasonic strengthening time is constant, the change in Young's modulus is unstable increasing ultrasonic strengthening pressure.

3.4 Effect of ultrasonic strengthening on elongation

To investigate the effects of ultrasonic strengthening parameters on the plastic mechanical properties of 3D printed samples, the elongations at the tensile strength and break were analyzed. Figure 12 and Fig. 13 show the tensile strength elongation of 3D printed samples for different ultrasonic strengthening parameters. The tensile strength elongation of the samples after ultrasonic strengthening does not change significantly. However, with increasing energy input into the samples, the error of the tensile strength elongation of the samples decreases significantly. This is mainly because, as the inner part of the printing samples becomes denser, the rasters are bonded more firmly. The strain is more stable when the samples reach uniform tensile strength.

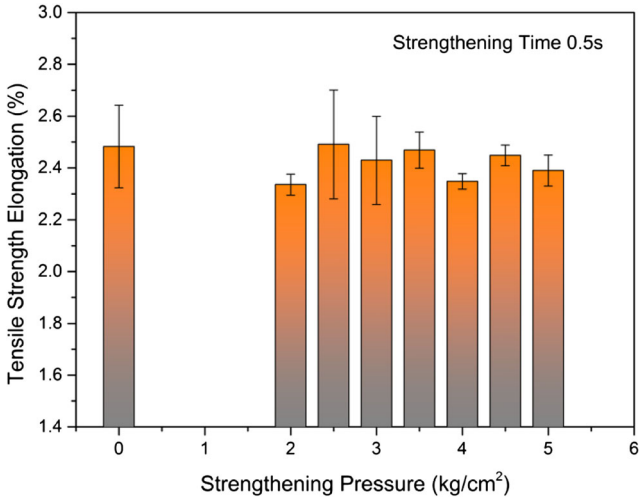

Fig. 13 Tensile elongation at ultrasonic strengthening time of 0.5 s

The ultimate elongation of 3D printed samples under different ultrasonic strengthening parameters is shown in Fig. 14 and Fig. 15. The ultimate elongation is slightly decreased after ultrasonic strengthening. However, with increasing energy input, the tensile strength increases, and the ultimate elongation does not show a downward trend. The results show that ultrasonic strengthening increases the strength and slightly decreases the ultimate elongation of samples. After the samples reach the tensile limit, they begin to produce crazing. As the strain increases further, the stress remains unchanged, and the crazing begins to widen until the samples break. The surface of the sample in contact with the horn was effected more strongly by ultrasonic vibrations, and printing defects near it were magnified. When the crazing widens, the rasters in this area break more easily, causing rapid fracture. This may be the main reason leading to the decrease of ultimate elongation. In addition, the surface of the samples becomes smoother after ultrasonic strengthening, so the surface texture of the untreated samples is relatively uneven. After the samples reach the yield limit, the uneven surface texture facilitates crazing, accelerating the fracture of the samples.

3.5 Characterization of ultrasonic strengthened 3D printed samples

Figure 16 shows micrographs of 3D printed samples. Figure 16a and Fig. 16A show that, in the untreated 3D printed

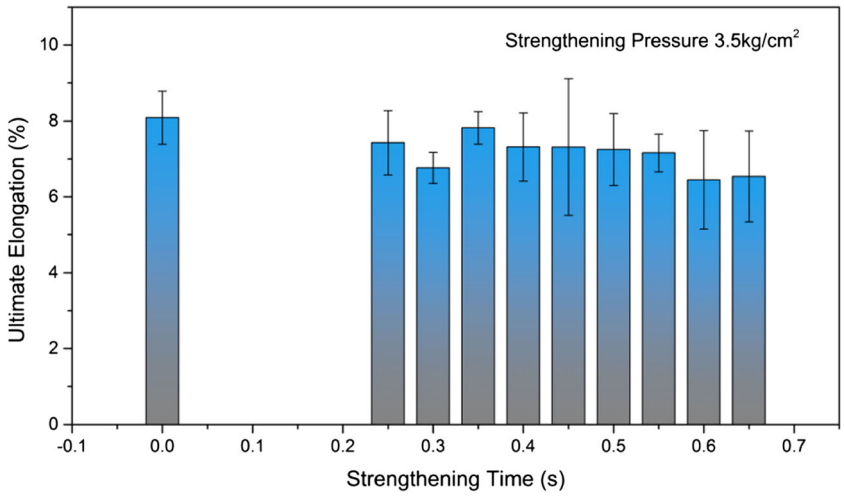

Fig. 14 Ultimate elongation under ultrasonic strengthening pressure of 3.5 kg/cm^2

samples, printed defects inside are distributed evenly, and the outline of the deposition boundary is clear. Figure 16b and Fig. 16B show that after 0.25 s of ultrasonic strengthening, the material on the side of work surface has become fused. With increasing ultrasonic strengthening time, the energy input to the samples increases gradually, and the fusion zone expands. Figure 16c and Fig. 16C show that when the ultrasonic strengthening time is 0.35 s, the fusion zone is larger than that in Fig. 16b. Moreover, the fusion among the rasters has become more uniform, and the single-yarn fracture is difficult to distinguish in the fusion zone. In the tensile test, the 3D printed sample is subjected to a tensile load at constant speed. The load per unit area of the sample increases gradually with increasing tensile displacement. When the force per unit area reaches the tensile limit of the weakest material in the sample, plastic deformation occurs and expands gradually. When the sample enters the plastic deformation state, the tensile strength of the sample reaches the maximum. After ultrasonic strengthening, the fusion zone is equivalent to a huge raster or injection-molded body. As the fusion zone increases, the load required for the unit displacement of elongation increases. As shown in Fig. 12 and Fig. 13, the tensile strength and elongation of the 3D printed samples show no obvious change; that is, the tensile displacement required by the weakest material in the samples is similar to the tensile limit. Therefore, the tensile mechanical properties of the samples are improved. With increasing of strengthening time, the fusion area continues to increase. However, as the strengthening time increases, the continuous vibrations cause printing defects near the surface in contact with the horn to expand. Figure 16d and Fig. 16D shows that, when the ultrasonic strengthening time is 0.45 s, there are large gaps near the surface in contact with the horn, and crazing occurs easily when under tension. With the expansion of crazing, the whole sample reaches the tensile limit. At this point, the ultrasonic strengthened samples become weaker, but remain stronger than the untreated samples. When the fusion zone grows closer to the surface in contact with the horn, the internal defects expanded by ultrasonic vibrations are fused and repaired, gradually strengthening the samples further. Figure 16e and Fig. 16E shows that, when the ultrasonic strengthening time is 0.65 s, the whole sample is almost completely fused, and only small 3D printing defects remain near the horn.

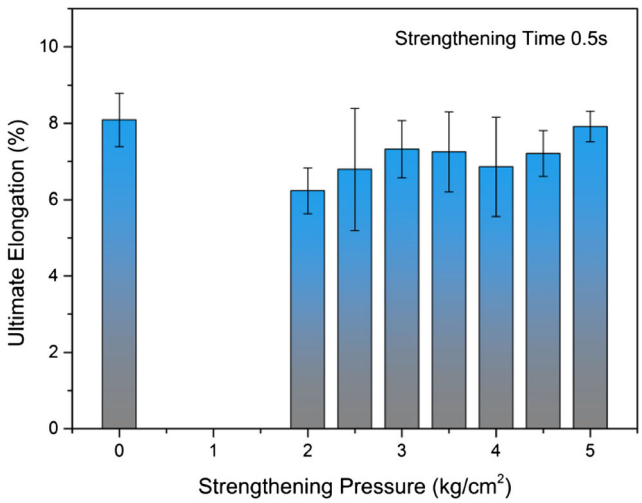

Fig. 15 Ultimate elongation under ultrasonic strengthening time of 0.5 s

Figure 17 shows the surface morphology of the untreated 3D printed sample. The surface of the untreated 3D printed sample surface is clear, with obvious stripes, and the surface height difference of the sample is 25.3 μm. Figure 18 shows the surface morphology of an ultrasonic strengthened sample. It is more difficult to see the stripes in some areas of the sample surface, and the height difference of the sample surface is 22.3 μm. The surface of ultrasonic strengthened sample is smoother than that of the untreated sample.

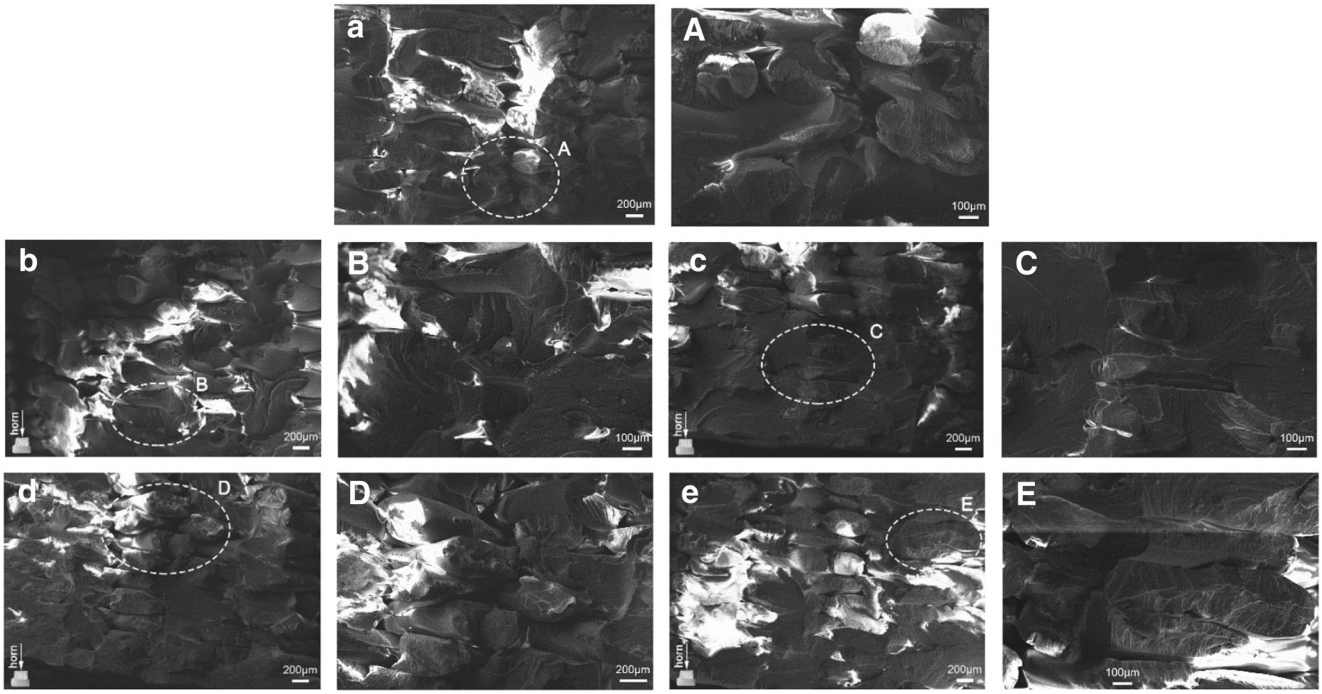

Fig. 16 Scanning electron microscopy images of **a** untreated 3D printed samples and 3D printed samples exposed to ultrasonic strengthening for **b** 0.25 s, **c** 0.35 s, **d** 0.45 s, and **e** 0.65 s, and **A**–**E** enlarged views of the corresponding areas

4 Conclusion

In this study, the effects of ultrasonic strengthening pressure and ultrasonic strengthening time on the tensile mechanical properties of FDM 3D printed ABS samples were studied. The control variable method was used to analyze the samples. The experimental results were analyzed and stress–strain curves of samples compared. The fracture characteristics of ultrasonic strengthened samples and untreated samples were compared using micrographs. The results show that defects in a 3D printed sample begin to fuse from the work surface side during ultrasonic strengthening. As the fusion area expands, the printing defects near the surface in contact with the horn expand, weakening the effect of ultrasonic strengthening. When the fusion zone grows closer to the contact surface of the horn, the enlarged defects are repaired by fusion, and the mechanical properties of the sample gradually improve until all defects are fully repaired. Ultrasonic strengthening of FDM 3D printed ABS samples enhances the mechanical properties of the samples significantly if appropriate ultrasonic strengthening parameters are chosen. This is helpful for promoting the application and development of FDM technology. Owing to the limitations of the ultrasonic strengthening system used in the research, the effects of strengthening for long times and at

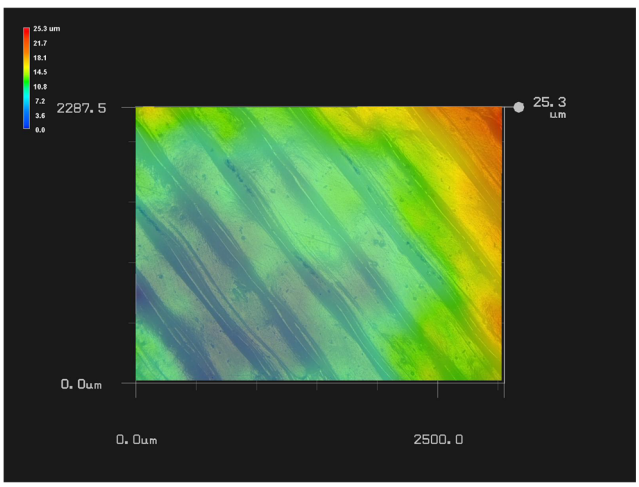

Fig. 17 Surface morphology of an untreated 3D printed sample

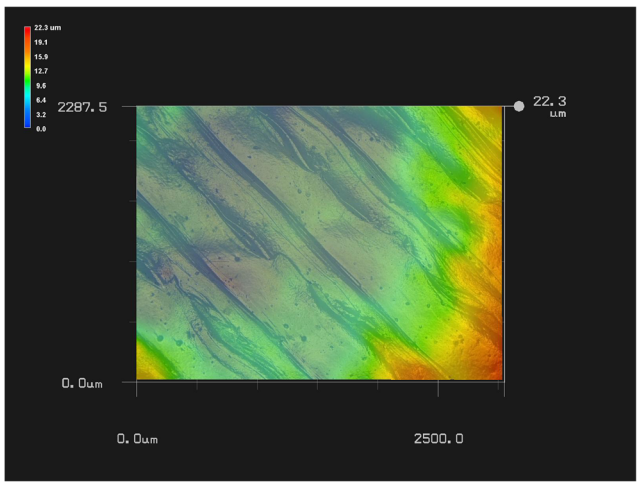

Fig. 18 Surface morphology a 3D printed sample following ultrasonic strengthening for 0.45 s at 3.5 kg/cm^2

high pressures were not studied. These effects will be studied in future after improving the ultrasonic strengthening system.

Acknowledgements This research is supported by National Natural Science Foundation of China (No. 51675226), Key Scientific and Technological Research Project of Jilin Province (No. 20180201055GX), Project of International Science and Technology Cooperation of Jilin Province (No. 20170414043GH), and Graduate Innovation Fund of Jilin University (No. 2017143).

References

1. Boschetto A, Veniali F (2010) Intricate shape prototypes obtained by FDM. Int J Mater Form 3(S1):1099–1102. https://doi.org/10.1007/s12289-010-0963-1
2. Chen L, He Y, Yang Y, Niu S, Ren H (2016) The research status and development trend of additive manufacturing technology. Int J Adv Manuf Technol 89(9–12):3651–3660. https://doi.org/10.1007/s00170-016-9335-4
3. MacDonald E, Wicker R (2016) Multiprocess 3D printing for increasing component functionality. Science 353(6307):aaf2093. https://doi.org/10.1126/science.aaf2093
4. Jin Y-A, He Y, Xue G-H, Fu J-Z (2014) A parallel-based path generation method for fused deposition modeling. Int J Adv Manuf Technol 77(5–8):927–937. https://doi.org/10.1007/s00170-014-6530-z
5. Wu WZ, Geng P, Zhao J, Zhang Y, Rosen DW, Zhang HB (2014) Manufacture and thermal deformation analysis of semicrystalline polymer polyether ether ketone by 3D printing. Mater Res Innov 18(sup5):S5-12–S15-16. https://doi.org/10.1179/1432891714z.000000000898
6. Yaman U (2017) Shrinkage compensation of holes via shrinkage of interior structure in FDM process. Int J Adv Manuf Technol 94:2187–2197. https://doi.org/10.1007/s00170-017-1018-2
7. Dawoud M, Taha I, Ebeid SJ (2016) Mechanical behaviour of ABS: an experimental study using FDM and injection moulding techniques. J Manuf Process 21:39–45. https://doi.org/10.1016/j.jmapro.2015.11.002
8. Stansbury JW, Idacavage MJ (2016) 3D printing with polymers: challenges among expanding options and opportunities. Dent Mater 32(1):54–64. https://doi.org/10.1016/j.dental.2015.09.018
9. Wu W, Geng P, Li G, Zhao D, Zhang H, Zhao J (2015) Influence of layer thickness and raster angle on the mechanical properties of 3D-printed PEEK and a comparative mechanical study between PEEK and ABS. Materials 8(9):5834–5846. https://doi.org/10.3390/ma8095271
10. Rebaioli L, Fassi I (2017) A review on benchmark artifacts for evaluating the geometrical performance of additive manufacturing processes. Int J Adv Manuf Technol 93(5–8):2571–2598. https://doi.org/10.1007/s00170-017-0570-0
11. Jin Y-A, Li H, He Y, Fu J-Z (2015) Quantitative analysis of surface profile in fused deposition modelling. Add Manuf 8:142–148. https://doi.org/10.1016/j.addma.2015.10.001
12. Ning F, Cong W, Qiu J, Wei J, Wang S (2015) Additive manufacturing of carbon fiber reinforced thermoplastic composites using fused deposition modeling. Compos Part B 80:369–378. https://doi.org/10.1016/j.compositesb.2015.06.013
13. Tian X, Liu T, Yang C, Wang Q, Li D (2016) Interface and performance of 3D printed continuous carbon fiber reinforced PLA composites. Compos A: Appl Sci Manuf 88:198–205. https://doi.org/10.1016/j.compositesa.2016.05.032
14. Nikzad M, Masood SH, Sbarski I (2011) Thermo-mechanical properties of a highly filled polymeric composites for fused deposition modeling. Mater Des 32(6):3448–3456. https://doi.org/10.1016/j.matdes.2011.01.056
15. Weng Z, Wang J, Senthil T, Wu L (2016) Mechanical and thermal properties of ABS/montmorillonite nanocomposites for fused deposition modeling 3D printing. Mater Des 102:276–283. https://doi.org/10.1016/j.matdes.2016.04.045
16. Lederle F, Meyer F, Brunotte G-P, Kaldun C, Hübner EG (2016) Improved mechanical properties of 3D-printed parts by fused deposition modeling processed under the exclusion of oxygen. Prog Addit Manuf 1(1–2):3–7. https://doi.org/10.1007/s40964-016-0010-y
17. Mohamed OA, Masood SH, Bhowmik JL (2016) Experimental investigation of the influence of fabrication conditions on dynamic viscoelastic properties of PC-ABS processed parts by FDM process. IOP Conf Ser: Mater Sci Eng 149:012122. https://doi.org/10.1088/1757-899x/149/1/012122
18. Suresh KS, Rani MR, Prakasan K, Rudramoorthy R (2007) Modeling of temperature distribution in ultrasonic welding of thermoplastics for various joint designs. J Mater Process Technol 186(1–3):138–146. https://doi.org/10.1016/j.jmatprotec.2006.12.028
19. Harun WSW, Sharif S, Idris MH, Kadirgama K (2013) Characteristic studies of collapsibility of ABS patterns produced from FDM for investment casting. Mater Res Innov 13(3):340–343. https://doi.org/10.1179/143307509x441513
20. Nuñez PJ, Rivas A, García-Plaza E, Beamud E, Sanz-Lobera A (2015) Dimensional and surface texture characterization in fused deposition modelling (FDM) with ABS plus. Procedia Eng 132:856–863. https://doi.org/10.1016/j.proeng.2015.12.570
21. Jami H, Masood SH, Song WQ (2013) Dynamic response of FDM made ABS parts in different part orientations. Adv Mater Res 748:291–294. https://doi.org/10.4028/www.scientific.net/AMR.748.291
22. Sahoo SK, Sahu AK, Mahapatra SS (2017) Environmental friendly electroless copper metallization on FDM build ABS parts. Int J Plast Technol 21:297–312. https://doi.org/10.1007/s12588-017-9185-4